Carbohydrate Polymers 98 (2013) 321–330

Contents lists available at SciVerse ScienceDirect

Carbohydrate Polymers

journal homepage: www.elsevier.com/locate/carbpol

Rheology and dynamic light scattering of octa-ethyleneglycol-monododecylether/chitosan solutions

Z.M. dos Santos, M.R. Pereira, J.L.C. Fonseca*

Instituto de Química, Universidade Federal do Rio Grande do Norte, Campus Universitário, Lagoa Nova, Natal, RN 59072-970, Brazil

ARTICLE INFO

Article history:
Received 25 March 2013
Received in revised form 28 May 2013
Accepted 31 May 2013
Available online 7 June 2013

Keywords:
Chitosan-surfactant interactions
Rheology
Dynamic light scattering
Relaxation rate distribution

ABSTRACT

In this work we used rheometry and DLS to probe relaxation phenomena in solutions of chitosan and octa-ethyleneglycol-monododecylether. The dispersions had a marked pseudoplastic behavior, which became less evident, as surfactant concentration was increased. Arrhenius plots showed that systems with surfactant presented a characteristic temperature at which apparent enthalpy of activation (varying from 3 to 40 kJ mol^{-1}) changed: this change was correlated to a possible transition of colloidal aggregates to a wormlike configuration. DLS intensity correlation functions were described by KWW equation: pure chitosan solutions had relaxation rate distributions centered at a characteristic relaxation rate around 4.6×10^{-6} μS^{-1}; as surfactant was added, a new component, with a faster characteristic relaxation rate with a magnitude order of 10^{-3} μs^{-1}, appeared. It was shown that the dependence between these relaxation rates and surfactant concentration could be used to describe DLS-related relaxation phenomena as an Arrhenius-activated process, agreeing with results obtained using rheometry.

1. Introduction

An appropriated knowledge of the interactions between polymers and surfactants provides one with the tools to appropriately control the rheology of many dispersed systems for different applications, from blood drag reduction for biomedical engineering (Malcher & Gzyl-Malcher, 2012) to oil exploration (Liu et al., 2012). These interactions are usually probed *via* surface tensiometry (Taylor, Thomas, & Penfold, 2007), rheometry (Bu, Kjoniksen, Elgsaeter, & Nystrom, 2006) and scattering techniques (Saxena, Antony, & Bohidar, 1998). Indeed, dynamic light scattering has been used to investigate the properties of colloids both in lyophobic and lyophilic forms, from inorganic nanoparticles (Murdock, Braydich-Stolle, Schrand, Schlager, & Hussain, 2008) to microbiological systems (Kouyianou et al., 2011), passing by polymer-based and surfactant-based dispersions (Einaga, 2009; Pecora, 2000).

C_nE_m surfactants are a very interesting object of study *per se*, as they have the property of forming colloidal aggregates with globular or wormlike geometries, depending on temperature and system composition, as it has been both experimentally and theoretically shown (Bulut, Hamit, Olsson, & Kato, 2008; Lauw, Leermakers, & Stuart, 2003; Moitzi, Freiberger, & Glatter, 2005). In fact, it has recently been reported the use of dynamic light scattering to characterize wormlike-globular geometry transition in $C_{12}E_9$-based microemulsions as a function of surfactant concentration (da Silva, Rossi, Neto, Dantas, & Fonseca, 2011) and temperature (da Silva, de Morais, Neto, Dantas, & Fonseca, 2012). Surfactant solutions containing wormlike structures present a great similarity with polymer solutions, wormlike micelles resembling polymer coils: because of that, properties such as intrinsic viscosity have been determined for these surfactants, when in solution (Shirai, Yoshimura, & Einaga, 2006). The interactions between these structures and polymers form, therefore, a very interesting field of study, both in practical and purely academic terms (Walker, 2009). The superposition of these fields is clearly represented by the work of van der Kooji et al., which have used DLS in conjunction with static techniques to characterize coacervate formation based on spherical and wormlike micelles using poly(acrylic acid) and an ethoxylated cationic polyelectrolyte (van der Kooij et al., 2012).

If one thinks of polymer–nonionic surfactant interactions in aqueous solutions, these very interactions are enhanced if the solubilized macromolecule has hydrophobic regions, these regions being, or not, a result of chemical modification (Che, Tan, Ren, Xin, & Meng, 2012). That makes chitosan, which has a surface activity of its own (Elsabee, Morsi, & Al-Sabagh, 2009), an interesting candidate for the study of these particular interactions. As commercial chitosan is the result of deacetylation of chitin, a natural polysaccharide, present in exoskeletons of crustaceans (Muzzarelli, Greco, Busilacchi, Sollazzo, & Gigante, 2012; Rocha, Dantas, Fonseca, & Pereira, 2002), the residual acetylated regions of chitosan may work as hydrophobic sites (Nystrom, Kjoniksen, & Iversen, 1999). When

* Corresponding author. Tel.: +55 84 3211 9224; fax: +55 84 3211 9224.
E-mail address: jlcfonseca.br@gmail.com (J.L.C. Fonseca).

0144-8617/$ – see front matter © 2013 Elsevier Ltd. All rights reserved.
http://dx.doi.org/10.1016/j.carbpol.2013.05.092

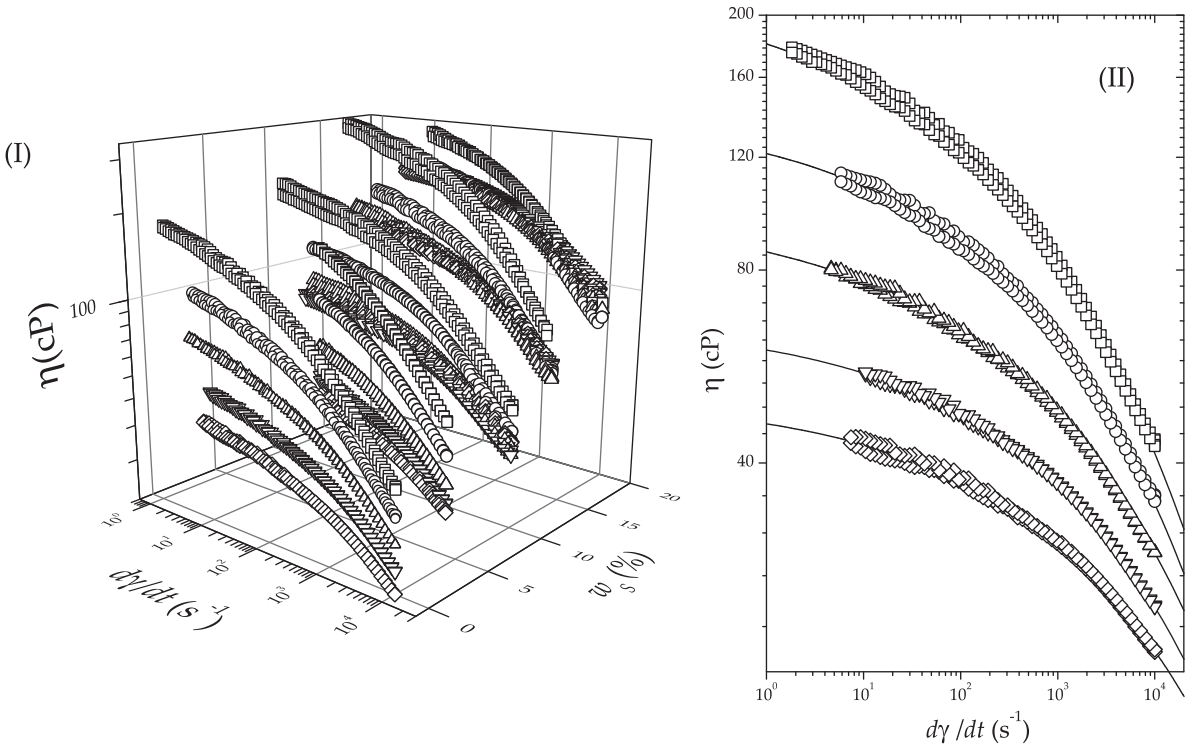

Fig. 1. (I) apparent viscosity, η, as a function of shear rate, $\dot{\gamma} = d\gamma/dt$, for chitosan/$C_{12}E_8$ solutions with different surfactant contents, w_S, and at different temperatures, T; (II) apparent viscosity as a function of shear rate for 2% chitosan solutions at different temperatures. Squares, $T = 10\,^{\circ}C$; circles, $T = 20\,^{\circ}C$; up-triangles, $T = 30\,^{\circ}C$; down-triangles, $T = 40\,^{\circ}C$; diamonds, $T = 50\,^{\circ}C$; continuous lines, Eq. (7).

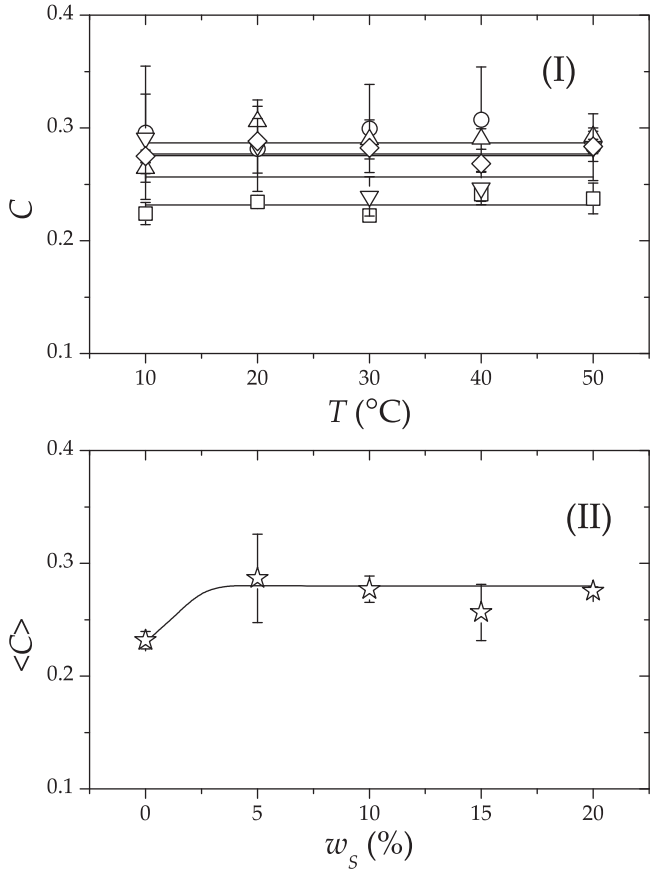

Fig. 2. (I) C, from Eq. (7), as a function of temperature for the chitosan/surfactant dispersions used in this work: squares, $w_S = 0\%$; circles, $w_S = 5\%$; up-triangles, $w_S = 10\%$; down-triangles, $w_S = 15\%$; diamonds, $w_S = 20\%$. (II) Temperature-averaged C, $\langle C \rangle$, as a function of surfactant content, w_S.

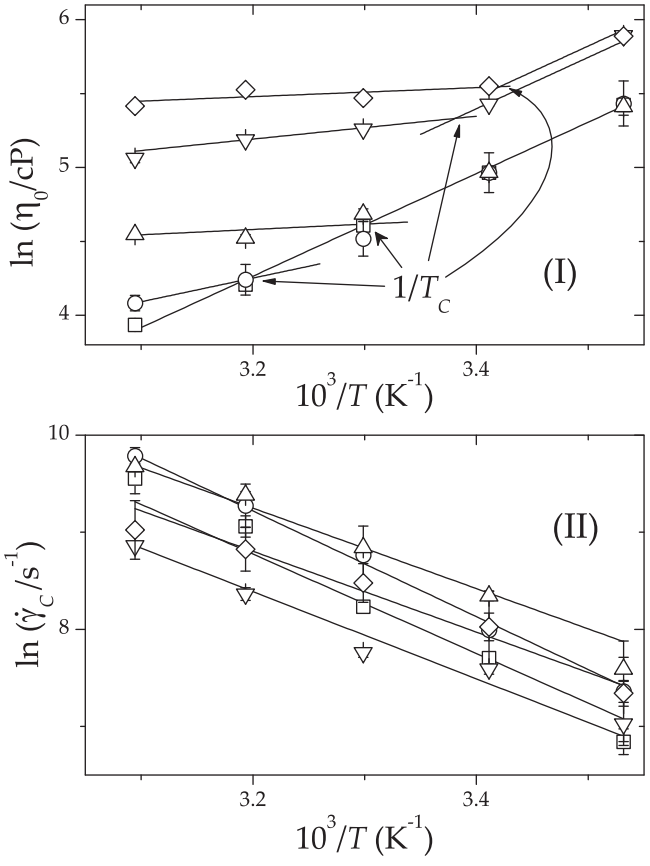

Fig. 3. (I) Arrhenius plot of zero-shear rate viscosity: squares, $w_S = 0\%$; circles, $w_S = 5\%$; up-triangles, $w_S = 10\%$ °C; down-triangles, $w_S = 15\%$; diamonds, $w_S = 20\%$; continuous lines, Eq. (8). (II) Arrhenius plot of $\dot{\gamma}_c$: squares, $w_S = 0\%$; circles, $w_S = 5\%$; up-triangles, $w_S = 10\%$; down-triangles, $w_S = 15\%$; diamonds, $w_S = 20\%$; continuous lines, Eq. (9).

working with dispersions containing chitosan, dynamic light scattering has mainly been used in the determination of nanoparticle dimensions of systems destined to (or with potential to be used in) controlled drug release (Juntapram, Praphairaksit, Siraleartmukul, & Muangsin, 2012) and the formation of self-assembled structures from chitosan-based copolymers (Bian, Jia, Yu, & Liu, 2009; Jiang, Quan, Liao, & Wang, 2006; Li, Yuan, Gu, & Ren, 2010; Yuan, Zhao, Gu, Ren, & Ren, 2011). Some few works have been carried out with chitosan in the form of a hydrophilic colloid, *e.g.*, using DLS to follow chitosan crosslinking in solution (de Morais, Pereira, & Fonseca, 2012), and to determine the dependence of relaxation phenomena in chitosan solutions on temperature and chitosan concentration (de Oliveira, de Morais, Pereira, & Fonseca, 2012).

The aim of this work is to use dynamic light scattering, associated to rheological measurements, to monitor relaxation processes occurring in chitosan-$C_{12}E_8$ solutions, *via* the determination of parameters related to the their relaxation rate distributions, as a function of surfactant concentration and temperature.

2. Experimental

Chitosan used in this work was purchased from Polymar LTD (Brazil). It had a deacetylation degree of 88% [determined by CHN elemental analysis and conductometric titration as described elsewhere (dos Santos, Caroni, Pereira, da Silva, & Fonseca, 2009)), intrinsic viscosity $[\eta] = 0.360\,g\,L^{-1}$, and average viscometric molar mass, $\bar{M}_v = 1.6 \times 10^5\,g\,mol^{-1}$ [determined using Mark–Houwink–Sakurada equation (Neto et al., 2005; Rinaudo, Milas, & Ledung, 1993)]. Acetic acid (P.A., Cromato Produtos Químicos LTD, Brazil), and octa-ethyleneglycol-monododecylether ($C_{12}E_8$, Ultrol L80, Oxiteno, Brazil) were used as received. Bi-distilled water was used in all experiments.

A chitosan/surfactant solution sample was prepared by mixing appropriate amounts of chitosan and surfactant to a 2% (m/v) acetic acid solution, in order to have 30 mL of dispersion. The resultant solution was left under stirring for 24 h, filtered through a 0.42 μm Millipore membrane filter and then taken to analysis.

Chitosan concentration was kept constant [2% (*m*/*v*)] and the following variables were analyzed:

- Surfactant mass content, w_S: 0%, 5%, 10%, 15%, and 20%.
- Temperature, T: 10 °C, 20 °C, 30 °C, 40 °C, and 50 °C.

2.1. Rheometry

Apparent dispersion viscosity (η) was determined at different shear rates, $\dot{\gamma} = d\gamma/dt$ (where γ is the shear strain), using a Haake Mars rheometer (Germany, cup DG 41 and rotor DG 41 DIN 5344).

2.2. Dynamic light scattering

DLS can be used to probe dynamic processes occurring in dispersions using the intensity correlation function, $g^{(2)}(t_D)$ (Degiorgio & Piazza, 1996; Shibayama, 1998, 2006):

$$g^{(2)}(t_D) \equiv g^{(2)}(t_D, q) = \frac{\langle I(0;q)I(t_D)\rangle_t}{\langle I(0;q)\rangle_t^2} \quad (1)$$

where t_D is the delay time, $I(t_D;q)$ is the scattered intensity at time t_D, q is the scattering vector modulus, $\langle i \rangle_t$ denotes a time average of i, and $g^{(2)}(t_D)$ is the scattering field time–correlation function.

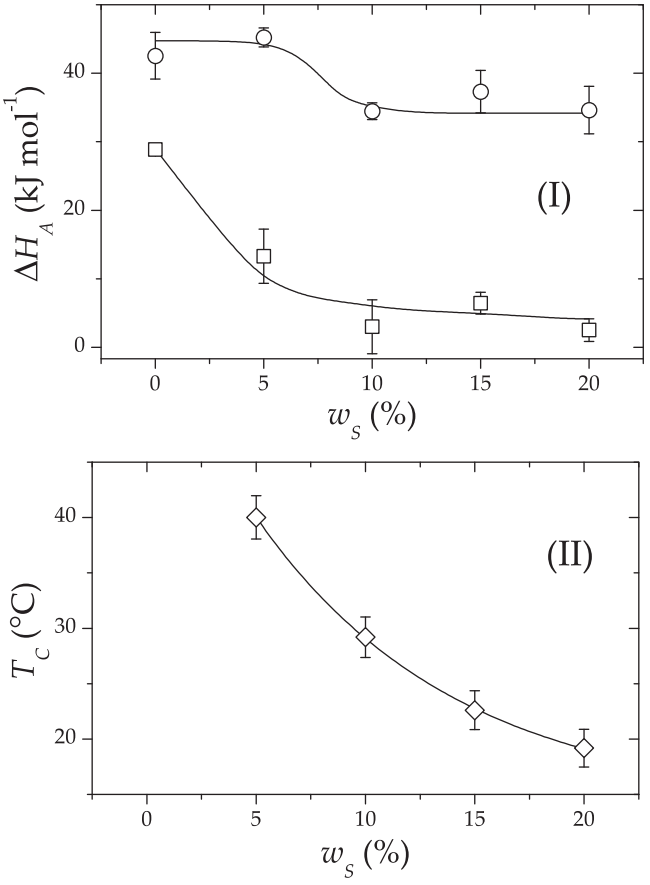

Fig. 4. (I) Apparent enthalpy of activation, ΔH_A, as a function of surfactant content, w_S: squares, ΔH_A calculated from η_0, Fig. 3(I); circles, calculated from $\dot{\gamma}_c$, Fig. 3(II). (II) Critical temperature, T_C, as a function of w_S [data withdrawn from Fig. 3(I)].

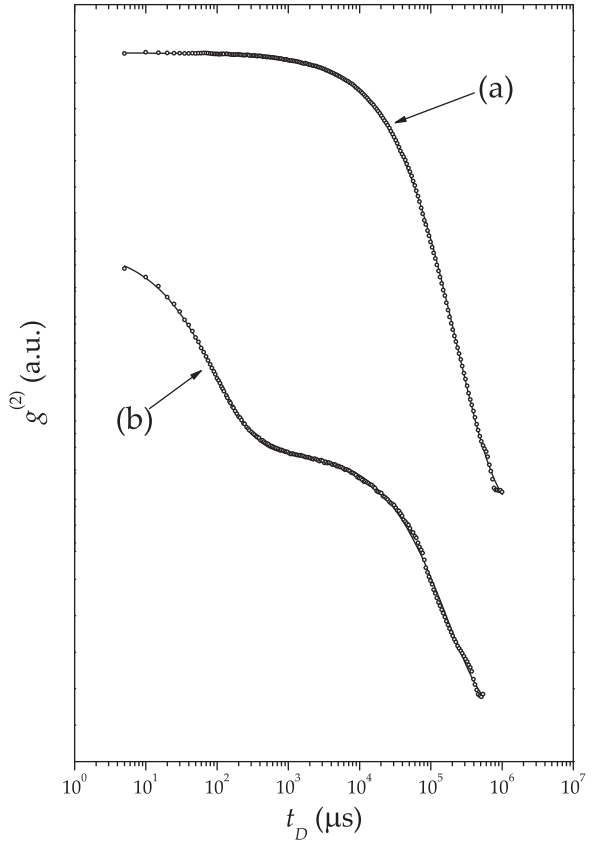

Fig. 5. Correlation intensity functions (ICF) of two samples: (I) chitosan solution at 20 °C with $w_S = 0$, and (II) with $w_S = 5\%$. Continuous lines, Eq. (11).

The intensity correlation function (ICF) $g^{(2)}$ is related to $g^{(1)}$, the theoretical field autocorrelation function, according to

$$g^{(2)}(t_D) = 1 + \beta\left[g^{(1)}(t_D)\right]^2 \quad (2)$$

where β is a constant that depends on the optical properties of the system. If there is a well defined, discrete, relaxation process, $g^{(1)}$ is

$$g^{(1)}(t_D) = e^{-\Gamma t_D} \quad (3)$$

where the relaxation rate, Γ, is

$$\Gamma = q^2 D \quad (4)$$

and

$$q = \frac{4\pi n_0}{\lambda} \sin\left(\frac{\theta}{2}\right). \quad (5)$$

D is the diffusion coefficient associated with this motion, n_0 is the refractive index of the sample, θ is the angle at which the detector is located to the sample cell, and λ is the radiation wavelength. If the relaxation process is better represented as a continuous relaxation rate distribution function, $G(\Gamma)$, Eq. (3) becomes

$$g^{(1)}(t_D) = \int_0^\infty G(\Gamma) e^{-\Gamma t_D}\, d\Gamma \quad (6)$$

The determination of $G(\Gamma)$, or parameters associated to analytical functions related to $g^{(1)}(t_D)$ or $g^{(2)}(t_D)$ yields information on the dynamics of these systems.

Dynamic light scattering experiments were carried out using a 90 Plus Particle Analyzer (Brookhaven Instruments Corporation, USA). Data acquisition parameters were adjusted as: time of analysis, 3 min (average of 3 measurements of 1 min); wavelength, 659 nm; scattering angle, $\theta = 90^\circ$.

3. Results and discussion

Before analyzing any result, we have to specify what are the conditions of the macromolecular coils in terms of flow regime. In order to quantify them, we use the dimensionless concentration $c^* = [\eta]c$, where $c = 20\ \mathrm{g\,L^{-1}}$ is the chitosan concentration and $[\eta] = 0.360\ \mathrm{g\,L^{-1}}$ is the chitosan intrinsic viscosity, which yields a value of $c^* = 7.2$. Since when $c^* \geq 6$ macromolecular coils are completely overlapped, *i.e.*, they are said to be in the concentrated regime (de Vasconcelos, de Azevedo, Pereira, & Fonseca, 2000; Launay, Cuvelier, & Martinez-Reyes, 1997).

3.1. Rheometry

Fig. 1(I) shows a plot of apparent viscosity, η, as a function of shear rate, $\dot{\gamma} = d\gamma/dt$, for different surfactant concentrations, w_s, and temperatures. From this figure, one can easily realize that:

- Apparent viscosity decreases as shear rate increases. This has been observed in micellar systems, dispersions, and polymer solutions (de Vasconcelos, Pereira, & Fonseca, 2005): it is related to the breakage of intermolecular interactions by shearing, a typical behavior of pseudoplastic fluids.
- For a fixed shear rate, apparent viscosity decreases as temperature is increased: it is related to the thermal breakage of intermolecular interactions (Wu, 2009). As shear rate is

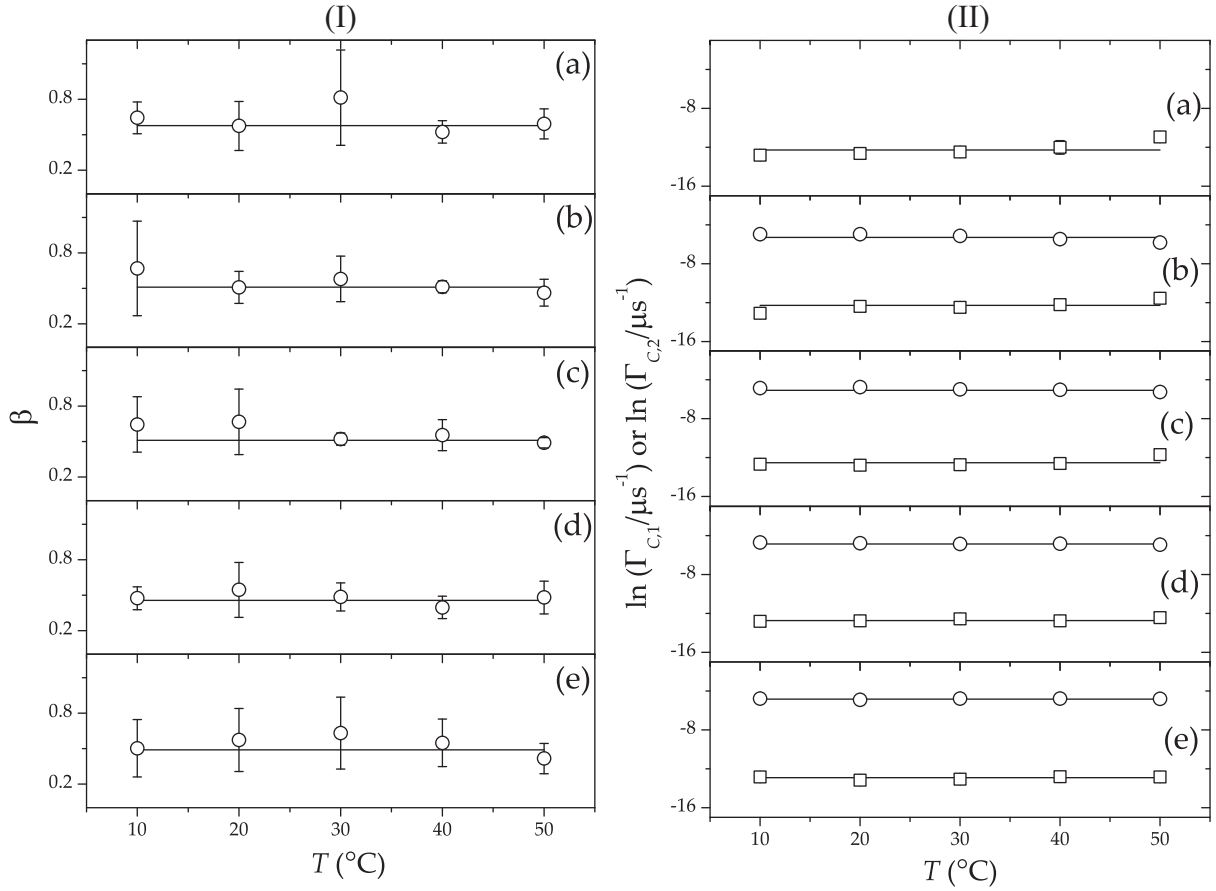

Fig. 6. (I) Parameter β, from Eq. (11), as a function of temperature, for different surfactant concentrations, w_S, and (II) logarithm of parameters $\Gamma_{C,1}$ (squares) and $\Gamma_{C,2}$ (circles), from Eq. (11), as a function of w_S: (a) $w_S = 0$; (b) $w_S = 5\%$; (c) $w_S = 10\%$; (d) $w_S = 15\%$; (e) $w_S = 20\%$.

increased, the decrease in apparent viscosity as temperature is increased is less evident, certainly due to the effect of shearing breakage of intermolecular interactions prior to thermal breakage by temperature increase.
- Finally, the increase in surfactant content results in a decrease in the effect of both temperature and shear rate on apparent viscosity. As a matter of fact, for the highest surfactant concentration used in this work (20%) the decrease in apparent viscosity is minimal at higher shear rates.

It seems, therefore, that the addition of $C_{12}E_8$ induces the formation of structures that minimize the action of both shear and temperature, decreasing the pseudoplastic character of the resultant dispersions. As pointed out in the introduction section, surfactants of the type C_nE_m may form colloidal tubular structures, the so-called wormlike micelles. As these micelles behave as macromolecular chains, their interaction with chitosan chains may result in physical crosslinking of it (or, using an alternative point of view, in physical crosslinking of polymer-mimicking wormlike micelles by chitosan). As a result, this more crosslinked system would not be so influenced by temperature and/or shear rate.

In order to analyze these factors in a more quantitative way, apparent viscosity and shear rate were correlated using the following empirical relationship:

$$\eta = \eta_0 e^{-(\dot{\gamma}/\dot{\gamma}_C)^C} \quad (7)$$

Eq. (7) has the form of a Kohlrausch–William–Watts stretched exponential function and fitted well to the data obtained in this work, as exemplified in Fig. 1(II), and has been used in the analysis of stress relaxation experiments (Monteiro & Fonseca, 1997) and dynamic light scattering data (da Silva et al., 2012; de Morais et al., 2012). By comparison, one could suggest the following physical meanings for the parameters of Eq. (7):

- η_0 is the value of apparent viscosity as $\dot{\gamma} \to 0$ (the so-called zero-shear rate viscosity);
- $\dot{\gamma}_c$ indicates the shear rate at which the decay in apparent viscosity is more noticeable: the stronger the interactions within the fluid are, the higher $\dot{\gamma}_c$ will be;
- C expresses the dependence of apparent viscosity on shear rate: as $C \to 0$, the relative fall in apparent viscosity, as shear rate is increased, tends to zero (at any shear rate).

Fig. 2(I) shows the dependence between C and temperature for the dispersions analyzed in this work. Although our experiments were not sensitive enough to detect a dependence between C and temperature, a dependence between its T-averaged value, $\langle C \rangle$, and surfactant content, w_S, can be observed in Fig. 2(II). The increase in $\langle C \rangle$ from *ca.* 0.23 to *ca.* 0.28, as surfactant is added to the solution, results in apparent viscosity being more influenced by shearing, *i.e.* surfactant addition induces the occurrence of structures that can be broken by shearing. This is consistent with a higher presence of wormlike micelles interacting with chitosan, as surfactant is present.

Zero-shear rate viscosity, η_0, presented a peculiar Arrhenius dependence on temperature, as shown in Fig. 3(I). More specifically, both situations may be described using Eyring's theory of viscous flow (de Vasconcelos, Bezerril, Pereira, Ginani, & Fonseca, 2011):

$$\ln\ \eta_0 = \ln A_1 + \frac{\Delta H_A}{RT} \quad (8)$$

where R is the universal gas constant, ΔH_A is the enthalpy of activation, $\ln A_1 = \ln A_0 - \frac{\Delta S_A}{RT}$, ΔS_A is the entropy of activation, and A_0 is a pre-exponential factor.

It can be seen that at a characteristic temperature, T_C, the slope of the straight line that describes the logarithmic dependence of viscosity on reciprocal temperature abruptly changes: it has a higher value below T_C than it has above this temperature: in fact it has the same value found for pure chitosan solution. The occurrence of T_C only happens if there is surfactant added to the system (pure 2% chitosan solution behavior is described by a curve with a single and constant slope): it indicates that the addition of surfactant resulted in the formation of structures that can be thermally broken at a characteristic temperature T_C. Indeed, we have suggested that T_C defines the point at which there is a discontinuity in the curve that can be related to a wormlike-sphere transition (da Silva et al., 2012).

The characteristic parameter, $\dot{\gamma}_c$, also has an Arrhenius-dependence on temperature, as shown in Fig. 3(II), following an Arrhenius dependence similar to Eq. (8), in the form of

$$\ln\ \dot{\gamma}_C = \ln A_1 - \frac{\Delta H_A}{RT} \quad (9)$$

Here, $\ln A_1 = \ln A_0 + \frac{\Delta S_A}{RT}$. In this case we did not observe an unequivocally defined critical temperature, T_C. That could be a result of either shearing at this characteristic shear rate having destroyed formed structures before T_C or preserving these very structures by orientation driven by shearing. The possibility of experimental uncertainty related to the parameters preventing the characterization of the discontinuity must not be ruled out. The same behavior has been reported for a microemulsion based on $C_{12}E_9$ nonionic surfactant (da Silva et al., 2012).

Fig. 4(I) displays the values of activation enthalpy, ΔH_A, as a function of surfactant concentration, w_S, obtained from η_0 and $\dot{\gamma}_c$, using Eq. (8) and Eq. (9), respectively. The first point to be noticed is

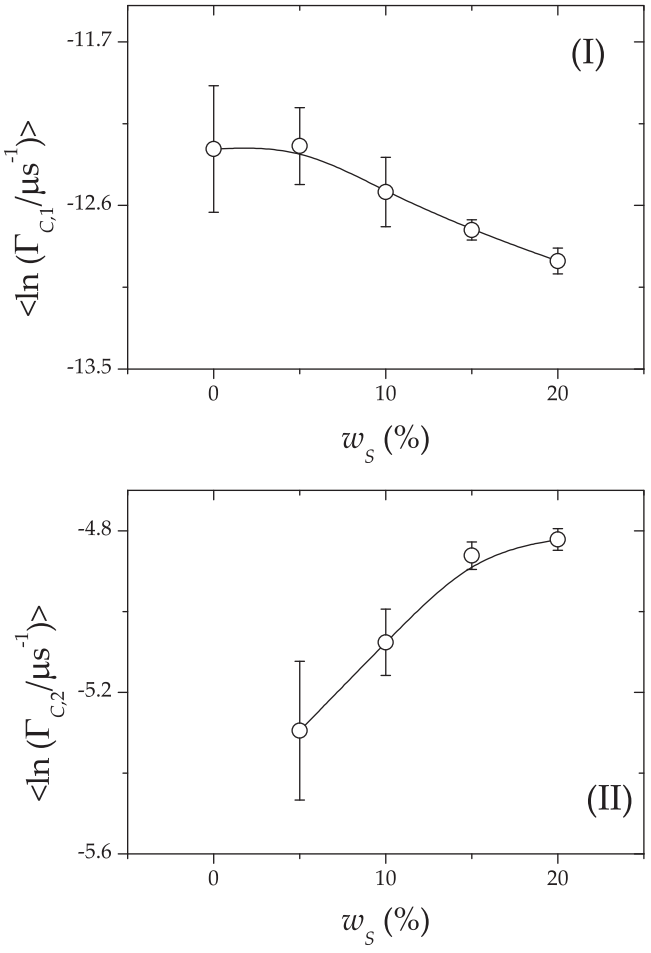

Fig. 7. (I) Temperature averaged $\ln \Gamma_{C,1}$, $\langle \ln \Gamma_{C,1} \rangle$, as a function of surfactant concentration, w_S, and (II) temperature averaged $\ln \Gamma_{C,2}$, $\langle \ln \Gamma_{C,2} \rangle$, as a function of w_S.

that ΔH_A has lower values for η_0: it markedly decays as surfactant concentration is increased. It is consistent with the state of the system at zero-shear rate conditions being more populated by weaker interactions, which are thermally broken more easily. As surfactant concentration is increased, ΔH_A decreases in both cases. This may have two interpretations:

- As the number of surfactant molecules is increased, polymer–polymer interactions become less important than weaker surfactant-polymer or surfactant–surfactant interactions.
- It has been shown that since chitosan has acetylated, nonpolar, regions, the increase in temperature will make chitosan chains to expand in a polar medium such as water (consistent with an endothermic solubilization process) (de Oliveira et al., 2012; de Vasconcelos et al., 2011). As chitosan chains are more expanded in solution, both intermolecular chitosan–chitosan and chitosan–surfactant interactions will be favored, (including interactions between nonpolar regions of chitosan, resultant from hydrophobic effect). If surfactant concentration is increased, by its turn, hydrophobic interactions between lipophilic regions of surfactant molecules and hydrophobic regions of chitosan macromolecules *via* hydrophobic effect will result in transformation of hydrophobic regions of chitosan into hydrophilic ones, resulting in further macromolecular expansion. Macroscopically, all these interactions will decrease the dependence between viscosity and temperature, *i.e.*, will yield lower values of ΔH_A.

Finally, one can verify in Fig. 4(II) that T_C continuously decreases as surfactant content is increased. As surfactant concentration is increased, the probability of surfactant–surfactant interactions (which means formation of wormlike micelles) increases: as these interactions tend to be weaker than surfactant–polymer and polymer–polymer ones, there is a decrease in the temperature at which these structures are thermally broken.

3.2. Dynamic light scattering

Intensity correlation functions (ICF) for pure chitosan solutions had the behavior described in a previous paper, following a one-staged process of decaying (de Oliveira et al., 2012), while as surfactant was added to the system the decay followed a two-stage behavior as already observed in another work with $C_{12}E_9$-based microemulsions (da Silva et al., 2012). This behavior is exemplified in Fig. 5, which shows ICF for a pure chitosan solution and for the same system with the addition of surfactant at $w_S = 5\%$, both at 20 °C. A composed Kohlraush–William–Watts equation has been used to describe this behavior (da Silva et al., 2012):

$$g^{(1)} = f_1 e^{-(\Gamma_{C,1} t_D)^{\nu}} + (1 - f_1) e^{-(\Gamma_{C,2} t_D)^{\nu}} \quad (10)$$

where $\Gamma_{C,1}$ is a characteristic relaxation rate for a given process 1, $\Gamma_{C,2}$ is a characteristic relaxation rate for a given process 2, and f_1 (which is between 0 and 1) gives the intensity by which process 1 operates.

The substitution of Eq. (10) in (2) yields

$$g^{(2)} = 1 + \beta \left[f_1 e^{-(\Gamma_{C,1} t_D)^{\nu}} + (1 - f_1) e^{-(\Gamma_{C,2} t_D)^{\nu}} \right]^2 \quad (11)$$

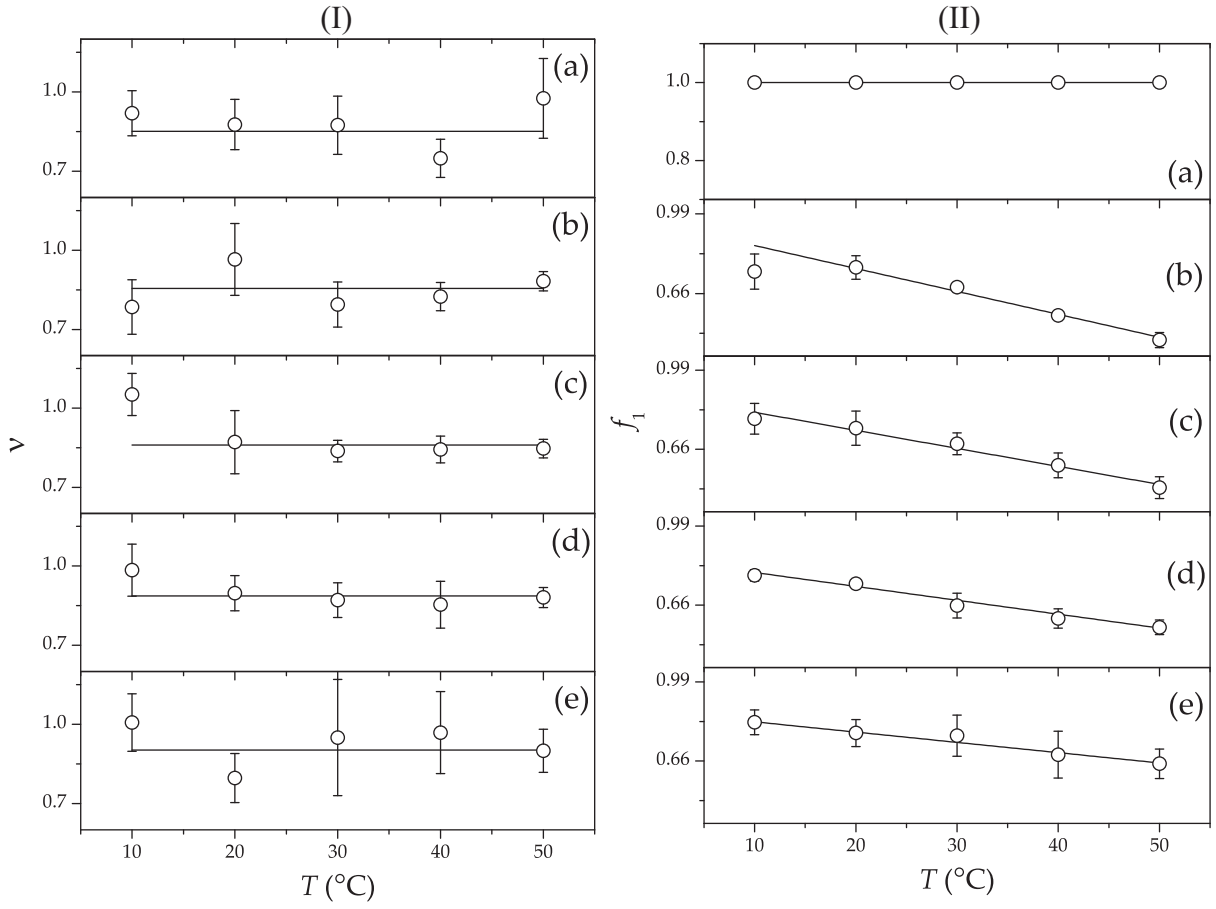

Fig. 8. (I) Parameter ν, from Eq. (11), as a function of temperature for different surfactant concentrations, w_S, and (II) parameter f_1, from Eq. (11), as a function of temperature for different surfactant concentrations, w_S: (a) $w_S = 0$; (b) $w_S = 5\%$; (c) $w_S = 10\%$; (d) $w_S = 15\%$; (e) $w_S = 20\%$; continuous lines, Eq. (12).

Eq. (11) was fitted to each of the sextuplicates of the ICF's obtained for each concentration and temperature and the resultant averaged parameter values will be discussed in the next paragraphs.

Fig. 6(I) shows the variation of β as a function of temperature for the samples used in this work. It can be seen that β was a function neither of temperature, T, nor surfactant concentration, w_S. If one has in mind that β is strongly influenced by crosslinking, abruptly decaying as it occurs (de Morais et al., 2012; Joosten, Geladé, & Pusey, 1990; Norisuye, Shibayama, Tamaki, & Chujo, 1999; Shibayama, 1998; Shibayama & Norisuye, 2002), the non-variable nature of β, therefore, clearly shows the non-crosslinked (chemically or physically) nature of the systems studied in this work.

Fig. 6(II) shows the dependence of the two relaxation rates, $\Gamma_{C,1}$ and $\Gamma_{C,2}$, on temperature, T, and surfactant content, w_S. It can be seen that, when comparing $\Gamma_{C,1}$ to $\Gamma_{C,2}$ in a logarithmic scale, the relaxation rates can be considered constant in relation to temperature. It can also be verified that for the pure chitosan solution, there is a characteristic relaxation rate with an order of magnitude of 10^{-6} μs^{-1}. As surfactant is added to the system, a new relaxation process seems to be present, with a characteristic relaxation rate with a magnitude order of 10^{-3} μs^{-1}. The appearance of a faster process must be correlated to the presence of interactions induced by structures that may be more easily (or fastly) broken as surfactant is added to the system. One can list the following reasons for it to happen:

- The interaction between the lipophilic part of the surfactant and nonpolar sites of chitosan will result in the substitution of hydrophobic interactions between chitosan chains by interactions that will be intermediated by surfactant interactions. In other words, surfactant molecules interact with hydrophobic sites of chitosan and the new polar sites of the surfactant molecules may interact with formed micelles, which result in structures that disentangle by faster processes.
- As surfactant concentration is increased, the presence of wormlike micelles is more and more favored. These structures, although similar to macromolecules, may be broken in a faster way than macromolecule-derived ones. In fact, the appearance of higher relaxation rates (or shorter relaxation times) has been reported as a result of the presence of supramolecular structures related to the increase in molecular weight during polymerization of styrene (Norisuye et al., 2005).

The dependence of T-averaged values of $\ln \Gamma_{C,1}$ and $\ln \Gamma_{C,2}$ ($\langle \ln \Gamma_{C,1} \rangle$ and $\langle \ln \Gamma_{C,2} \rangle$, respectively) on surfactant content, w_S, is shown in Fig. 7. An increase in w_S has opposite effects on relaxation rates: relaxation rate for slower processes decreases, while it increases for faster processes. The decrease in the characteristic relaxation rate for the slower processes must be linked to the increase in the difficulty of random movement of macromolecular chains, as these chains become immersed in an entangled network of chains made by increasingly longer wormlike micelles. On the other hand, if one think of surfactant by itself, as the increase in size of wormlike molecules results in longer structures, these precise structures may be more easily broken, resulting in bigger values of $\langle \ln \Gamma_{C,2} \rangle$.

Fig. 8(I) shows the dependence between the parameter ν from Eq. (11) and temperature for different surfactant contents. It is know that as $\nu \to 1$ the relaxation rate (or relaxation time) distribution tend to narrow to a defined, unique relaxation frequency, the opposite happening when $\nu \to 0$ (broadening of relaxation rate distribution) (da Silva et al., 2012; Monteiro & Fonseca, 1997). Fig. 8(I) indicates that ν is relatively constant, independent of temperature, *i.e.*, relaxation rate distribution width also seems not to change with temperature. It raises the following question: if Γ_C's and ν do not considerably change with temperature, why relaxation as a whole changes with temperature? The answer to this question is related to the parameter f_1: changes in relaxation behavior may be governed by changes in the importance of slow and fast relaxation processes. This can easily be demonstrated by an analysis of Fig. 8(II), which shows the dependence of f_1 with temperature for different surfactant concentrations. For pure chitosan solution, there is no such a dependence, of course, since $f_1 = 1$. As surfactant is added to the system, there is a decrease in f_1, indicating a higher importance of the faster relaxation processes. In fact, f_1 linearly decreases with temperature, following Eq. (12):

$$f_1 = f_0 - \alpha_f T \tag{12}$$

where f_0 is a constant and $-\alpha_f$ is the slope of Eq. (12). Consequently, as temperature is increased, interactions are broken and faster relaxation processes become more and more important.

Fig. 9 shows the dependences between the slopes α_f and the T-averaged values of ν, $\langle \nu \rangle$, on surfactant concentration, w_S. In terms of α_f, it can be seen that as surfactant is added, there is a sharp increase in it: this simply is due to the fact that, before surfactant is added f_1 is 1 at any T (which implies $\alpha_f = 0$). Further increase in surfactant content results in the decrease of α_f: As faster relaxation rate processes become more important, f_1 tends to decrease to a constant minimum value and its dependence on temperature, of course, will be minimized as well. On the other hand, $\langle \nu \rangle$ continuously increases with w_S, indicating that interactions become more homogeneous

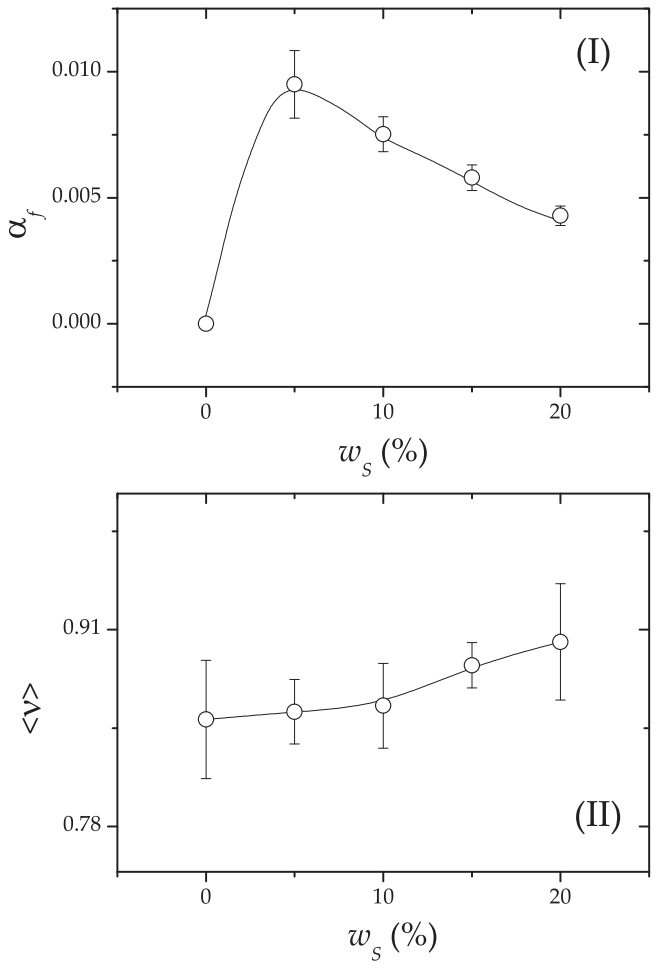

Fig. 9. (I) α_f as a function of surfactant concentration, w_S, for the dispersions used in this work. (II) Average values of ν, $\langle \nu \rangle$ (taken from Fig. 8(I)), as a function of w_S.

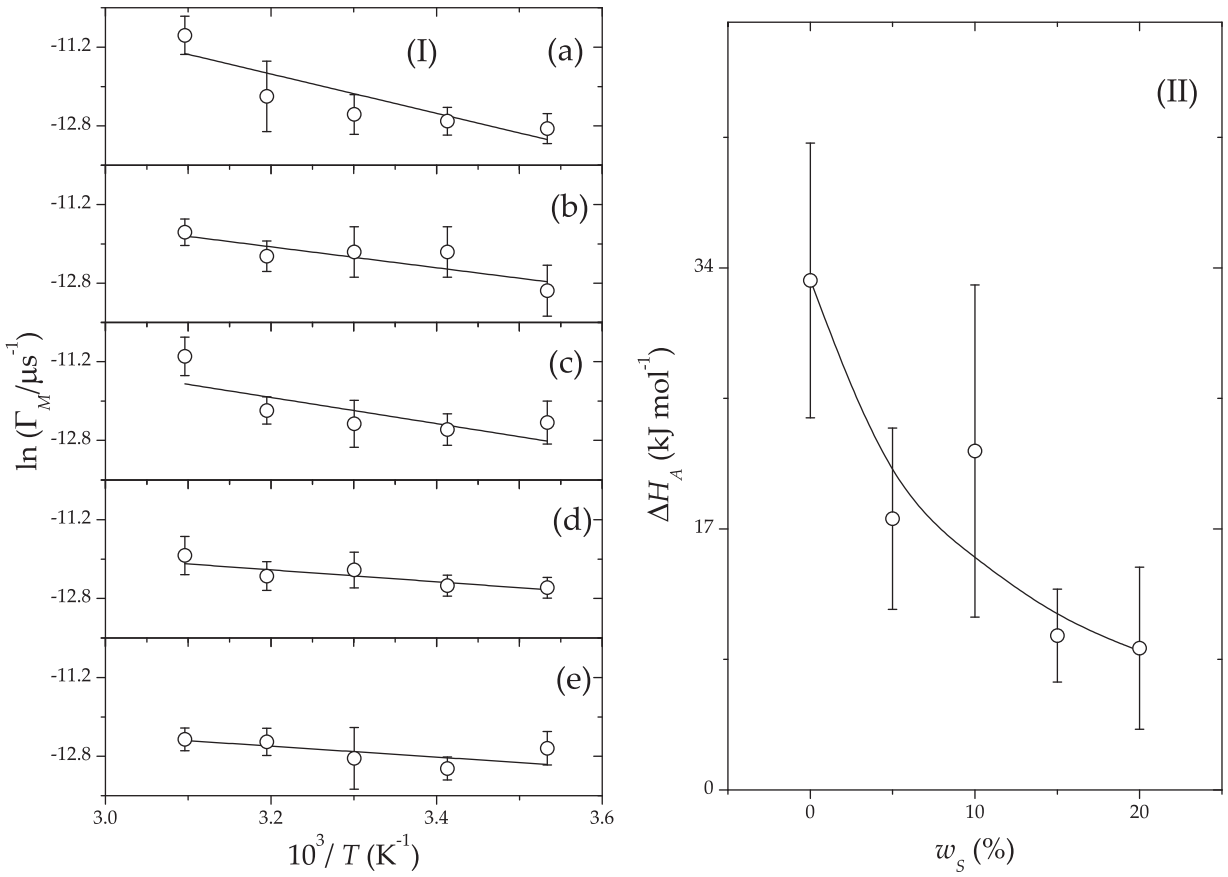

Fig. 10. (I) Logarithm of Γ_M, from Eq. (15), as a function of reciprocal absolute temperature, T: (a) $w_S = 0$; (b) $w_S = 5\%$; (c) $w_S = 10\%$; (d) $w_S = 15\%$; (e) $w_S = 20\%$; continuous lines, Eq. (17). (II) (I) Enthalpy of activation, ΔH_A, obtained from data from this figure and Eq. (17).

as surfactant content is increased. This is consistent with $C_{12}E_8$ micelles "filling the gaps" between chitosan macromolecular chains, ruling interactions within the solution, resulting in a distribution of relaxation rates more homogeneous (chitosan–water and chitosan–chitosan interactions would be less important).

The effect of temperature could be better explored if the distribution of relaxation rates were analyzed as an activated process. To do this, we can use an approach already employed to analyze relaxation time distributions: in this case the dependence between an average relaxation time and temperature is the object of analysis (Choi & Kwak, 2004; Pich, Schiemenz, Boyko, & Adler, 2006). In the same way it has been reported for a process with a single relaxation time, for a single relaxation rate Γ one has that

$$\int_0^\infty g^{(1)}(t_D)\,dt_D = \int_0^\infty e^{-\Gamma t_D}\,dt_D = \frac{1}{\Gamma} \tag{13}$$

An average relaxation rate, Γ_M, may analogously be defined as

$$\Gamma_M = \frac{1}{\int_0^\infty g^{(1)}(t_D)\,dt_D} \tag{14}$$

Substitution of (10) in (14) yields

$$\Gamma_M = \frac{\nu}{\Gamma_F(1/\nu)}\left(\frac{f_1}{\Gamma_{C,1}} + \frac{1-f_1}{\Gamma_{C,2}}\right) \tag{15}$$

where $\Gamma_F(1/\nu)$ is the gamma function of $1/\nu$:

$$\Gamma_F\left(\frac{1}{\nu}\right) = \int_0^\infty x^{1/\nu-1}e^{-x}\,dx \tag{16}$$

An activation energy-governed average relaxation rate may be defined, analogously to Eq. (9), as:

$$\ln \Gamma_M = \ln A_1 - \frac{\Delta H_A}{RT} \tag{17}$$

Fig. 10(I) shows that Eq. (17) is well fitted to the experimental data (within experimental errors) and the obtained values of ΔH_A for the chitosan solutions are displayed in Fig. 10(II).

In the same way it happened to η_0 and $\dot{\gamma}_c$, the decrease in ΔH_A, as w_S is increased, must be due to one (or both) the following reasons:

- The increase in the importance of faster relaxation processes results in a decrease in ΔH_A, since the related interactions are weaker.
- The decrease in ΔH_A simply express a lower dependence between average relaxation rate and temperature, for the same reasons listed in the rheometry section. In the case of chitosan/$C_{12}E_8$ solutions, surfactant molecules in the wormlike conformation would enhance this effect, since worm micelle contour length, L, decreases with temperature according to (Varade, Rodriguez-Abreu, Delgado, & Aramaki, 2007)

$$L = \sqrt{\phi}e^{E_C/2kT} \tag{18}$$

where k is the Boltzmann constant, ϕ is the volume fraction of wormlike micelles and E_C is the end-cap energy. A small average contour length would imply a higher amount of free surfactant molecules, which would interact with non-polar regions of chitosan molecules. As a result, there would be a higher coil expansion, resulting in less intense decrease in average relaxation rate.

In the second analysis we have focused our attention on macromolecular coils (slow relaxation rate processes). In fact, the importance of slow relaxation rate processes in Γ_M becomes quite evident if we have in mind that $\Gamma_{C,2}$ is *ca.* 3 orders of magnitude bigger than $\Gamma_{C,1}$; if we re-write Eq. (15), having this consideration in mind:

$$\Gamma_M = \frac{\nu}{\Gamma_F(1/\nu)}\left(\frac{f_1}{\Gamma_{C,1}} + \frac{1-f_1}{\Gamma_{C,2}}\right)^{-1} \cong \frac{\nu}{\Gamma_F(1/\nu)}\left(\frac{f_1}{\Gamma_{C,1}}\right)^{-1} = \frac{\nu\Gamma_{C,1}}{f_1\Gamma_F(1/\nu)} \quad (19)$$

In other words, slower relaxation rate processes govern average relaxation rates, so that the second hypothesis for a smaller relaxation enthalpy must be the correct one.

Finally, if we compare Fig. 10(II) to Fig. 4(I), we can see that both the values and behavior of ΔH_A obtained from DLS and η_0 are in the same range: it reinforces the analysis carried out in this work, since in both cases one works with systems that are not under shear.

4. Conclusions

Flow activation enthalpies calculated from zero-shear rate viscosity indicates that the addition of $C_{12}E_8$ to chitosan solutions results in the occurrence of a second flow activation enthalpy in an atypical Arrhenius plot. DLS, by its turn, confirms the occurrence a second mode of viscous dissipation in the form of relaxation rate distributions centered at two characteristic relaxation rates. The contribution of slower relaxation rates mainly come from chitosan–chitosan interactions, while surfactant-related interactions govern faster relaxation processes. Fitting of ICF data to KWW equation showed that as surfactant content increased, relaxation processes became more homogeneous and temperature influence on relaxation decreased, mainly due to the fact that chitosan macromolecular coils were more expanded in solution. This higher expansion was the result of hydrophobic interactions between the nonpolar regions of chitosan and the decrease in the dimensions of wormlike micelles by increase of temperature (small micelles would be more accessible to interact with chitosan). All the results derived from rheometry strengthened these conclusions, in particular the similar dependence of the zero-shear rate viscosity and average relaxation rate-related activation enthalpies with surfactant concentration. The use of this sort of DLS–rheometry correlation to characterize surfactant–polymer interactions has not, to our knowledge, been reported in the literature and can be used to tune the rheological properties of these systems for a wide range of applications, such as viscosifiers for painting formulations, food hydrocolloids, and drilling fluids.

Acknowledgments

The authors thank Brazil's Conselho Nacional de Desenvolvimento Científico e Tecnológico (CNPq), Coordenação de Aperfeiçoamento de Pessoal de Nível Superior (CAPES), and Pró-Reitoria de Pesquisa da Universidade Federal do Rio Grande do Norte (PROPESQ-UFRN) for financial support during the course of this work.

References

Bian, F. L., Jia, L. X., Yu, W., & Liu, M. Z. (2009). Self-assembled micelles of N-phthaloylchitosan-g-polyvinylpyrrolidone for drug delivery. *Carbohydrate Polymers*, *76*(3), 454–459.

Bu, H. T., Kjoniksen, A. L., Elgsaeter, A., & Nystrom, B. (2006). Interaction of unmodified and hydrophobically modified alginate with sodium dodecyl sulfate in dilute aqueous solution—Calorimetric, rheological, and turbidity studies. *Colloids and Surfaces A: Physicochemical and Engineering Aspects*, *278*(1–3), 166–174.

Bulut, S., Hamit, J., Olsson, U., & Kato, T. (2008). On the concentration-induced growth of nonionic wormlike micelles. *European Physical Journal E*, *27*(3), 261–273.

Che, Y. J., Tan, Y. B., Ren, X. N., Xin, H. P., & Meng, F. J. (2012). Solution properties of hydrophobically modified acrylamide-based polysulfobetaines in the presence of surfactants. *Colloid and Polymer Science*, *290*(13), 1237–1245.

Choi, J., & Kwak, S. Y. (2004). Concentration fluctuation and cooperative chain mobility of hyperbranched poly(epsilon-caprolactone)s investigated by photon correlation spectroscopy. *Polymer*, *45*(21), 7173–7183.

da Silva, G. C., de Morais, W. A., Neto, A. A. D., Dantas, T. N. C., & Fonseca, J. L. C. (2012). The relationship between rheology and dynamic light scattering for a xylene/water/ButOH/C12E9 microemulsion. *Colloids and Surfaces A: Physicochemical and Engineering Aspects*, *397*, 42–47.

da Silva, G. C., Rossi, C. G. F. T., Neto, A. A. D., Dantas, T. N. C., & Fonseca, J. L. C. (2011). Characterization of wormlike micellar systems using DLS, rheometry and tensiometry. *Colloids and Surfaces A: Physicochemical and Engineering Aspects*, *377*(1–3), 35–43.

de Morais, W. A., Pereira, M. R., & Fonseca, J. L. C. (2012). Characterization of gelification of chitosan solutions by dynamic light scattering. *Carbohydrate Polymers*, *87*(4), 2376–2380.

de Oliveira, V. A. V., de Morais, W. A., Pereira, M. R., & Fonseca, J. L. C. (2012). Dynamic light scattering in semidilute and concentrated chitosan solutions. *European Polymer Journal*, *48*(11), 1932–1939.

de Vasconcelos, C. L., Bezerril, P. M., Pereira, M. R., Ginani, M. F., & Fonseca, J. L. C. (2011). Viscosity-temperature behavior of chitin solutions using lithium chloride/DMA as solvent. *Carbohydrate Research*, *346*(5), 614–618.

de Vasconcelos, C. L., de Azevedo, F. G., Pereira, M. R., & Fonseca, J. L. C. (2000). Viscosity-temperature-concentration relationship for starch-DMSO-water solutions. *Carbohydrate Polymers*, *41*(2), 181–184.

de Vasconcelos, C. L., Pereira, M. R., & Fonseca, J. L. C. (2005). Polyelectrolytes in solution and the stabilization of colloids. *Journal of Dispersion Science and Technology*, *26*(1), 59–70.

Degiorgio, V., & Piazza, R. (1996). Light scattering in colloid and interface science. *Current Opinion in Colloid & Interface Science*, *1*(1), 11–16.

dos Santos, Z. M., Caroni, A. L. P. F., Pereira, M. R., da Silva, D. R., & Fonseca, J. L. C. (2009). Determination of deacetylation degree of chitosan: a comparison between conductometric titration and CHN elemental analysis. *Carbohydrate Research*, *344*(18), 2591–2595.

Einaga, Y. (2009). Wormlike micelles of polyoxyethylene alkyl ethers CiEj. *Polymer Journal*, *41*(3), 157–173.

Elsabee, M. Z., Morsi, R. E., & Al-Sabagh, A. M. (2009). Surface active properties of chitosan and its derivatives. *Colloids and Surfaces B: Biointerfaces*, *74*(1), 1–16.

Jiang, G. B., Quan, D. P., Liao, K. R., & Wang, H. H. (2006). Preparation of polymeric micelles based on chitosan bearing a small amount of highly hydrophobic groups. *Carbohydrate Polymers*, *66*(4), 514–520.

Joosten, J. G. H., Geladé, E. T. F., & Pusey, P. N. (1990). Dynamic light-scattering by nonergodic media—Brownian particles trapped in polyacrylamide gels. *Physical Review A*, *42*(4), 2161–2173.

Juntapram, K., Praphairaksit, N., Siraleartmukul, K., & Muangsin, N. (2012). Electrosprayed polyelectrolyte complexes between mucoadhesive N,N,N, -trimethylchitosan-homocysteine thiolactone and alginate/carrageenan for camptothecin delivery. *Carbohydrate Polymers*, *90*(4), 1469–1479.

Kouyianou, K., De Bock, P. J., Muller, S. A., Nikolaki, A., Rizos, A., Krzyzanek, V., et al. (2011). The chlorosome of *Chlorobaculum tepidum*: Size, mass and protein composition revealed by electron microscopy, dynamic light scattering and mass spectrometry-driven proteomics. *Proteomics*, *11*(14), 2867–2880.

Launay, B., Cuvelier, G., & Martinez-Reyes, S. (1997). Viscosity of locust bean, guar and xanthan gum solutions in the Newtonian domain: A critical examination of the log ηsp – log C[η]0 master curves. *Carbohydrate Polymers*, *34*(4), 385–395.

Lauw, Y., Leermakers, F. A. M., & Stuart, M. A. C. (2003). Self-consistent-field prediction for the persistence length of wormlike micelles of nonionic surfactants. *Journal of Physical Chemistry B*, *107*(39), 10912–10918.

Li, X. F., Yuan, W. Z., Gu, S. Y., & Ren, J. (2010). Synthesis and self-assembly of tunable thermosensitive chitosan amphiphilic copolymers by click chemistry. *Materials Letters*, *64*(24), 2663–2666.

Liu, J. X., Guo, Y. J., Hu, J., Zhang, J., Lv, X., Zhang, X. M., et al. (2012). Displacement characters of combination flooding systems consisting of gemini-nonionic mixed surfactant and hydrophobically associating polyacrylamide for bohai offshore oilfield. *Energy & Fuels*, *26*(5), 2858–2864.

Malcher, T., & Gzyl-Malcher, B. (2012). Influence of polymer-surfactant aggregates on fluid flow. *Bioelectrochemistry*, *87*, 42–49.

Moitzi, C., Freiberger, N., & Glatter, O. (2005). Viscoelastic wormlike micellar solutions made from nonionic surfactants: Structural investigations by SANS and DLS. *Journal of Physical Chemistry B*, *109*(33), 16161–16168.

Monteiro, E. E. C., & Fonseca, J. L. C. (1997). Phase segregation and viscoelastic behavior of poly(ether urethane urea)s. *Journal of Applied Polymer Science*, *65*(11), 2227–2236.

Murdock, R. C., Braydich-Stolle, L., Schrand, A. M., Schlager, J. J., & Hussain, S. M. (2008). Characterization of nanomaterial dispersion in solution prior to In vitro exposure using dynamic light scattering technique. *Toxicological Sciences*, *101*(2), 239–253.

Muzzarelli, R. A. A., Greco, F., Busilacchi, A., Sollazzo, V., & Gigante, A. (2012). Chitosan, hyaluronan and chondroitin sulfate in tissue engineering for cartilage regeneration: A review. *Carbohydrate Polymers*, *89*(3), 723–739.

Neto, C. G. D., Fernandes, A. L. P., Santos, A. I. B., Morais, W. A., Navarro, M. V. M., Dantas, T. N. C., et al. (2005). Preparation and characterization of chitosan-based dispersions. *Polymer International*, *54*(4), 659–666.

Norisuye, T., Morinaga, T., Tran-Cong-Miyata, Q., Goto, A., Fukuda, T., & Shibayama, M. (2005). Comparison of the gelation dynamics for polystyrenes prepared by conventional and living radical polymerizations: a time-resolved dynamic light scattering study. *Polymer*, *46*(6), 1982–1994.

Norisuye, T., Shibayama, M., Tamaki, R., & Chujo, Y. (1999). Time-resolved dynamic light scattering studies on gelation process of organic–inorganic polymer hybrids. *Macromolecules*, *32*(5), 1528–1533.

Nystrom, B., Kjoniksen, A. L., & Iversen, C. (1999). Characterization of association phenomena in aqueous systems of chitosan of different hydrophobicity. *Advances in Colloid and Interface Science*, *79*(2–3), 81–103.

Pecora, R. (2000). Dynamic light scattering measurement of nanometer particles in liquids. *Journal of Nanoparticle Research*, *2*(2), 123–131.

Pich, A., Schiemenz, N., Boyko, V., & Adler, H. J. P. (2006). Thermoreversible gelation of biodegradable polyester (PHBV) in toluene. *Polymer*, *47*(2), 553–560.

Rinaudo, M., Milas, M., & Ledung, P. (1993). Characterization of chitosan - influence of ionic-strength and degree of acetylation on chain expansion. *International Journal of Biological Macromolecules*, *15*(5), 281–285.

Rocha, A. N. L., Dantas, T. N. C., Fonseca, J. L. C., & Pereira, M. R. (2002). Permeation of drugs in chitosan membranes. *Journal of Applied Polymer Science*, *84*(1), 44–49.

Saxena, A., Antony, T., & Bohidar, H. B. (1998). Dynamic light scattering study of gelatin-surfactant interactions. *Journal of Physical Chemistry B*, *102*(26), 5063–5068.

Shibayama, M. (1998). Spatial inhomogeneity and dynamic fluctuations of polymer gels. *Macromolecular Chemistry and Physics*, *199*(1), 1–30.

Shibayama, M. (2006). Universality and specificity of polymer gels viewed by scattering methods. *Bulletin of the Chemical Society of Japan*, *79*(12), 1799–1819.

Shibayama, M., & Norisuye, T. (2002). Gel formation analyses by dynamic light scattering. *Bulletin of the Chemical Society of Japan*, *75*(4), 641–659.

Shirai, S., Yoshimura, S., & Einaga, Y. (2006). Intrinsic viscosity of polyoxyethylene alkyl ether CiEj micelles. *Polymer Journal*, *38*(1), 37–43.

Taylor, D. J. F., Thomas, R. K., & Penfold, J. (2007). Polymer/surfactant interactions at the air/water interface. *Advances in Colloid and Interface Science*, *132*(2), 69–110.

van der Kooij, H. M., Spruijt, E., Voets, I. K., Fokkink, R., Stuart, M. A. C., & van der Gucht, J. (2012). On the stability and morphology of complex coacervate core micelles: From spherical to wormlike micelles. *Langmuir*, *28*(40), 14180–14191.

Varade, D., Rodriguez-Abreu, C., Delgado, J. G., & Aramaki, K. (2007). Viscoelasticity and mass transfer in phenol-CTAB aqueous systems. *Colloid and Polymer Science*, *285*, 1741–1747.

Walker, L. M. (2009). Scattering from polymer-like micelles. *Current Opinion in Colloid & Interface Science*, *14*(6), 451–454.

Wu, M. (2009). Shear-thinning and viscosity synergism in mixed solution of guar gum and its etherified derivatives. *Polymer Bulletin*, *63*(6), 853–863.

Yuan, W. Z., Zhao, Z. D., Gu, S. Y., Ren, T. B., & Ren, J. (2011). Synthesis and self-assembly of pH-responsive chitosan graft copolymer by the combination of atom transfer radical polymerization and click chemistry. *Materials Letters*, *65*(4), 793–796.